Online Detection of Railway Track Irregularities via JADE-Based Blind Source Separation and MEMS Accelerometry

Hongtao Zhang*, Guang Jin*, Na Zhang
Zhengzhou Railway Vocational and Technical College, Zhengzhou 451460, China
E-mail: zzrvtczht@126.com, jguang80@sina.com
*Corresponding author

Technical paper

Keywords: vibration mechanism features, vibration acceleration sensor, blind source separation algorithm, railway track, irregularity fault, detection system

Received: July 17, 2025

To address the difficulties in accurately capturing the characteristic changes of track irregularities in real - time and the limited ability to process complex mixed vibration signals, this study proposes an online Detection of Railway Track Irregularities via JADE-Based Blind Source Separation and MEMS Accelerometry. The system consists of a lower computer and an upper computer with ADXL345 three-axis acceleration sensor as the core. Real time track vibration signals are collected through optimized IIC bus protocol, and the blind source separation algorithm based on JADE is executed by STM32F103ZET6 microprocessor. By jointly diagonalizing the mixed vibration signal through a fourth-order cumulative matrix, the track roughness feature components in the mixed vibration signal are effectively decoupled, achieving accurate detection of railway track roughness. The detection results are converted into USB signals through RS-232 serial port and CH340G chip, and uploaded to the upper computer. The upper computer platform visualizes the type, location, and severity of track roughness faults. At the same time, a dual level power management and anti reverse protection are designed to ensure the reliability of the railway environment. To verify system performance, 8 monitoring points were set up on a 30-kilometer actual operating line, and multiple sets of vibration data were continuously collected at a sampling frequency of 10240 Hz at train speeds of 60-80 km/h. Establish the ground truth value of faults through high-precision track inspection vehicles and total station measurements, and compare it with HybridGAN method and data mining method. The experimental results show that this system can achieve an average positioning error of $\leqslant$ 1.8 mm, a fault type recognition accuracy of $\geqslant$ 96%, and an average detection time of $\leqslant$ 90 ms at a speed of 60 km/h. At a speed of 80 km/h, it still maintains an error of $\leqslant$ 2.2 mm and a recognition accuracy of $\geqslant$ 90%, with better performance than the two comparison methods. The upper computer of the system has the function of visualizing fault types, locations, and degrees, and integrates dual level power management and anti reverse protection, which is suitable for complex railway environments. This system provides a feasible solution for real-time monitoring of track status with high accuracy and low latency.

Povzetek: Študija predstavi sistem za sprotno zaznavanje nepravilnosti železniške proge z MEMS pospeškometrom in algoritmom slepe ločitve signalov JADE, ki omogoča zelo natančno in hitro odkrivanje tipa, lokacije in resnosti napak na progi.

1 Introduction

Railways, as an important infrastructure and mass transportation tool, have many advantages such as high capacity, low cost, high efficiency, and environmental friendliness, undertaking a large volume of passenger and freight transportation tasks [1]. However, with the rapid development of railway transportation, the increasing train speeds and load capacities pose more severe challenges to the track. Track irregularities have gradually become one of the key factors affecting the safety, comfort, and efficiency of railway transportation. Track irregularities refer to deviations in the geometric shape, dimensions, and spatial position of the track relative to its normal state. These deviations can cause intense vibrations and shocks during train operation [2], which not only accelerate the wear and damage of the track structure and shorten its service life but also affect the smoothness and safety of train operation. In severe cases, they may even lead to derailments and other major safety accidents. Therefore, real-time and accurate detection of railway track irregularities and the timely identification and handling of potential faults [3] are of great significance for ensuring railway transportation safety and improving transportation efficiency.

In order to promptly detect and address track irregularities, ensuring the safety and smoothness of railway transportation, many scholars have long proposed track inspection methods, such as Khasani R R and others who proposed an image quality enhancement method based on HybridGAN for automatic railway track defect recognition [4]. By collecting a large number of dynamically acquired railway inspection images, combining ESRGAN (used to improve image resolution) and DeblurGANv2 (used to reduce image blurriness), a HybridGAN model is constructed. The original dataset is used to train HybridGAN, enabling it to learn how to convert low-quality images into high-resolution, low-blurriness images, thereby clarifying the location and type of track faults in the images. However, this method only detects track faults from the perspective of image quality enhancement, neglecting other important information such as track vibrations. Stewart E and others proposed a track fault detection method based on Variational Mode Decomposition (VMD) [5]. This method decomposes the collected raw vibration signals using the VMD algorithm to obtain multiple intrinsic mode functions (IMFs) with different frequency characteristics. Based on each IMF obtained from the decomposition, the energy value is calculated to extract energy features related to track conditions. The signals to be tested undergo the same decomposition and feature extraction process before being input into a trained classifier to determine whether there is a fault and its type. However, this method only relies on energy features for track fault judgment, with low feature dimensionality, which may not comprehensively cover all information about track irregularities. Hany O and others proposed a data mining-based track fault detection method [6], combining Logical Data Analysis (LAD) with Ant Colony Optimization (ACO). First, ACO's search capability is used to explore key feature combinations related to high-impact loads within vast amounts of railway track historical data. Then, LAD performs logical analysis of these feature combinations to identify patterns that clearly distinguish high-impact loads from normal loads. Based on these patterns, a classification model is built to classify unknown observation data, achieving track fault detection. However, this method requires mining feature patterns from large datasets; if the data contains noise, missing values, or errors, it can affect the search results of ACO and the logical analysis of LAD, leading to an inaccurate classification model that cannot effectively detect track faults. Koohmishi M and others proposed a method that integrates Ground Penetrating Radar (GPR) and Synthetic Aperture Radar Interferometry (InSAR) technology, introducing machine learning models to achieve efficient track fault detection [7]. InSAR is used to obtain surface deformation data of the track area, reflecting changes in overall structural stability, while GPR scans the underlying structure of the track to acquire underground defect information. After preprocessing the collected data, features related to track faults are extracted separately, and the two sets of features are fused to form a more comprehensive feature vector. A machine learning model is then trained and used for classification to determine whether there is a fault and its type. However, the InSAR technology's accuracy is significantly affected by atmospheric conditions, satellite orbit errors, and other factors, which may lead to inaccurate fault detection results.

There is a close intrinsic relationship between vibration mechanism characteristics and track irregularities. When a train runs on an uneven track, the interaction forces between the wheel and rail change, causing vibrations in the vehicle and track structure [8]. Different types and degrees of track irregularities can induce specific vibration responses in the vehicle and track, which contain rich information about track irregularities [9]. Therefore, this article proposes online detection of railway track irregularities via jade-based blind source separation and MEMS accelerometry, with vibration signals generated by the interaction between train and track as the research object, is essential. By utilizing advanced vibration acceleration sensor technology and data analysis algorithms, real-time collection, processing, and analysis of track vibration signals can be performed to extract features related to track irregularities, achieving accurate detection and localization of track faults. This provides a new method for track condition monitoring for railway transportation departments, helping to improve the targeting and timeliness of track maintenance, reduce maintenance costs, and ensure the safe and efficient operation of railways.

One of the core objectives of this study is to verify a specific hypothesis: the blind source separation algorithm based on JADE can more effectively separate the feature components related to track roughness from complex wheel rail mixed vibration signals than traditional BSS signal processing methods, thereby achieving high-precision and low latency fault detection. Therefore, at the algorithmic level, this study specifically chose JADE because of its fourth-order cumulative quantity (high-order statistic) characteristics, which theoretically can better handle non-Gaussian distribution vibration source signals, and has faster convergence speed and higher separation accuracy than methods that rely only on second-order statistics or stochastic gradient optimization (such as FastICA). This is crucial for meeting the real-time and accuracy requirements of online detection. At the hardware level, the selection of sensor ADXL345 is based on its cost-effectiveness, compact packaging (easy to install and protect), and sufficient performance indicators: its ± 16g measurement range can cover the magnitude of track impact vibration, its 3.9mg/LSB high sensitivity can distinguish small roughness features, and its digital output and low power consumption characteristics greatly simplify the design of the lower computer system, making it very suitable for large-scale and distributed deployment along railways.

2 Online fault detection system for railway track irregularities

2.1 System design

During the operation of a train, the vibration signals generated by the wheel-rail interaction contain information about the geometric state of the track [10], such as vertical irregularities, alignment irregularities, and horizontal irregularities. Therefore, an online fault detection system for railway track irregularities based on vibration mechanism characteristics is designed. The system consists of a lower-computer system and an upper-computer node, as shown in Figure 1.

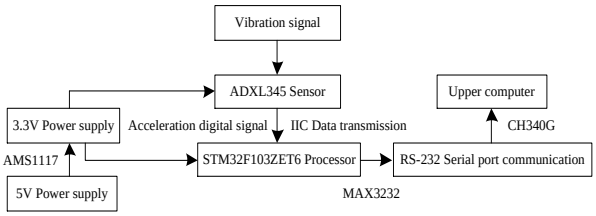

Figure 1: Schematic diagram of the system design.

Among them, the lower-computer system includes ADXL345 vibration acceleration sensor data acquisition, IIC real-time data transmission, microprocessor STM32F103ZET6, RS-232 wired communication, and a power supply module. The functions of each component of the system and the overall working process are as follows:

1) The ADXL345 vibration acceleration sensor can accurately collect the vibration signals of the track and digitize the collected analog vibration signals.

2) The digitized vibration signals from the ADXL345 are transmitted to the microprocessor STM32F103ZET6 in real-time through the IIC bus.

3) After receiving the vibration signals, the microprocessor STM32F103ZET6 processes and analyzes the vibration signals using a blind source separation method based on JADE (Joint Approximate Diagonalization of Eigenmatrices). It effectively separates the vibration signal components related to track irregularities, extracts useful feature information, and realizes the fault detection of railway track irregularities.

4) With the help of RS-232 serial communication and related conversion chips, the fault detection result data of railway track irregularities is sent to the upper-computer for display. Considering the limited number of computer serial ports, the system uses the RS-232 to USB chip CH340G for data transmission, converting RS-232 signals to USB signals for connection to the computer, so that the upper-computer can receive the fault detection result data.

5) After receiving the fault detection result data, the upper-computer displays it in an intuitive way, including information such as the type, position, and degree of track irregularities. This enables operators to timely understand the operating status of the track, detect potential fault hazards, and provide a decision-making basis for the maintenance and inspection of railway tracks.

6) The power supply hardware circuit includes two voltage regulator chips: the MP2359 DC-DC chip and the AMS1117 level conversion chip. DC_IN is used for external DC power input, which is converted into a 5V DC power output through the MP2359 DC-DC chip. By utilizing a reverse-connection protection diode, the circuit is safeguarded from damage in case of polarity confusion in the external DC power supply. The AMS1117 chip serves as a 5V-to-3.3V level conversion chip, providing 3.3V power support to the hardware circuit.

To expand the monitoring range and improve system performance, multiple lower-computer nodes work cooperatively. Each lower-computer node is responsible for collecting track vibration signals in a specific area, as well as processing and analyzing them. Multiple lower-computer nodes can share data and work cooperatively to jointly complete the fault detection task of railway track irregularities.

2.2 Data acquisition module design

In the system's data acquisition module, a MEMS (Micro-Electro-Mechanical Systems) based ADXL345 vibration acceleration sensor is selected as the core component. It is installed near the train wheelsets and key parts of the track using a secure attachment method to ensure accurate collection of effective vibration signals that reflect the track condition [11]. The ADXL345 vibration acceleration sensor is a three-axis digital output accelerometer composed of a differential capacitor and a surface-micromachined polysilicon structure. Under external acceleration, the polysilicon mechanism produces an offset that changes the capacitance value. This design is based on railway track engineering applications, which require strict sensitivity. The ADXL345 sensor has a maximum sensitivity of 3.9 mg/LSB and can measure tilt angles as small as 1.0°, fully meeting railway track engineering requirements. To simplify the design, the digital output accelerometer facilitates vibration signal data processing and analysis. Its power consumption is only 40~145 uA, and standby mode consumes only 0.1 uA, significantly reducing the overall energy consumption of the system, making the design more user-friendly and better suited for practical railway engineering applications.

In addition to selecting appropriate sensors, the installation position of the track vibration signal acquisition system is also crucial. The ADXL345 vibration acceleration sensor has a wide frequency response range, high reliability, and sensitivity. Incorrect installation can affect the results of railway track irregularity fault detection and may also cause hardware damage to the ADXL345 vibration acceleration sensor. Therefore, the installation location mainly considers the sensor's working environment and the vibration state of the measured track section. Generally, the following two principles should be followed:

(1) Positions with high stiffness and small structural damping should be chosen as the measurement points on the track.

(2) The measurement points on the track should be as close as possible to the vibration source.

The functional block diagram of the ADXL345 vibration acceleration sensor is shown in Figure 2. Its internal structure includes a three-axis sensor (3-AXIS SENSOR) responsible for detecting acceleration along the X, Y, and Z axes and converting it into analog signals. After preliminary processing by the sensing electronics circuit (SENSE ELECTRONICS CS), the signals are converted into digital signals by an analog-to-digital converter (ADC) and then denoised by a digital filter (DIGITAL FILTER). The processed data are stored in a 32-LEVEL FIFO buffer to reduce the load on the external processor. The serial input/output interface (SERIAL I/O) supports IIC and SPI protocols, facilitating communication with external devices. The power management (POWER MANAGEMENT NT) module supplies power to the chip, while the control and interrupt logic (CONTROL AND INTERRUPT LOGIC) module handles chip control and interrupt management.

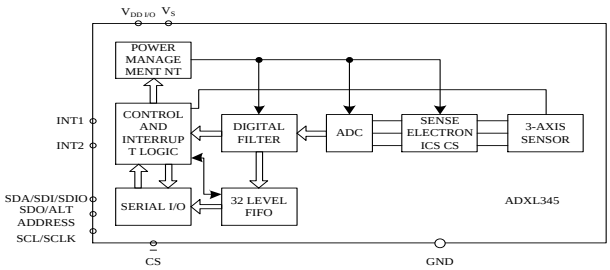

Figure 2: Functional block diagram of ADXL345.

In terms of operation, the ADXL345 vibration acceleration sensor sequentially completes the detection of railway track vibration signals, analog processing, analog-to-digital conversion, digital filtering, and data storage. When interacting with external devices, data can be transmitted via the IIC or SPI interface, and external devices can send commands to configure its working modes and other parameters. Interrupt conditions can also be set, and when met, interrupt signals are sent through the INT1 and INT2 pins. Additionally, external devices can perform batch reading of vibration signal data from the FIFO to improve the efficiency of railway track vibration signal acquisition [12].

2.3 Design of the real-time data transmission module

The system's real-time data transmission module is responsible for enabling data communication between the ADXL345 vibration accelerometer sensor and the STM32F103ZET6 microprocessor. Since the ADXL345 vibration accelerometer supports both SPI and IIC communication protocols, and the IIC protocol only requires two wires (data line SDA and clock line SCL) to achieve data transmission between master and slave devices, it significantly reduces the number of I/O ports used compared to the SPI protocol, thereby simplifying system design complexity and reducing costs. Therefore, the IIC communication protocol is adopted in the system's real-time data transmission module.

IIC bus interface structure design is shown in Figure 3, primarily comprising two parts: an internal frequency divider and an IIC bus interface control timing logic module. Typically, the external input clock frequency of an FPGA is relatively high, while IIC bus has specific data transmission rate requirements, with the standard mode operating at 100 kbit/s and the fast mode at 400 kbit/s. The internal frequency divider's function is to divide the high-frequency external clock signal, outputting a data transmission rate compliant with IIC bus requirements to meet the timing requirements for IIC bus data transmission. IIC bus interface control timing logic module serves as the control core of IIC bus interface module, generating all timing control logic for IIC bus data transmission, such as the generation of start and stop signals, addressing of the slave device (ADXL345), and the transmission and reception of data on the bus [13].

IIC bus port mapping and functions are shown in Table 1.

IIC bus interface module supports two basic data transmission modes: single-byte data write mode and single-byte data read mode. Since the module provides corresponding status information before, during, and after read/write operations (Start, Inter_Addr, Done, AckCointer), the host (microprocessor) can determine whether to perform the next byte data read/write operation based on this information, thereby enabling continuous read/write operations on the internal storage units of the slave device (ADXL345). This ultimately achieves four IIC bus data transmission operation modes: single-byte data write, single-byte data read, multi-byte data continuous write, and multi-byte data continuous read.

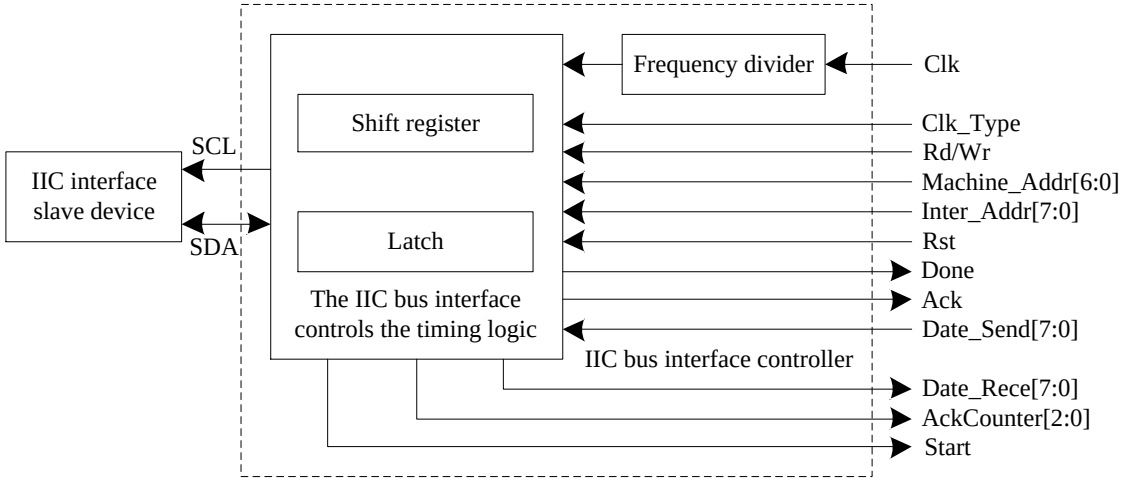

Figure 3: IIC bus interface structure.

Table 1: IIC bus port mapping and functions

Port	Function Description
Clk	External input clock of FPGA
Clk_Type	The SCL output clock mode: 0 is the standard mode and 1 is the fast mode
Rd/Wr	Read and write control signals: 1 represents the master reading data from the slave, and 0 represents the master writing data to the slave
Machine_Addr[6:0]	The unique address identifier from the machine part
Inter_Addr[7:0]	The address of the storage unit from which the machine part is to be operated
SCL	IIC bus interface clock line
Start	The start signal for the read and write operations of the interface module is indicated, and the falling edge is valid
Rst	The reset signal of the bus interface module is 0, which is valid
Done	When the host completes a read/write operation on the slave, the signal shows a falling edge; otherwise, it is at a high level
Ack	The response signal from the slave to the master
AckCounter[2:0]	The counter for the host to receive the response signal from the slave
SDA	IIC bus interface data cable
Date_Send[7:0]	The byte data sent by the host to the slave
Date_Received[7:0]	The host receives the byte data from the slave

2.4 Wired communication module design

In the system's data acquisition module, the results of fault detection for uneven railway tracks are transmitted to the upper computer display using RS-232 serial communication and related conversion chips [14]. The interface pins of RS-232 are defined as shown in Table 2.

Table 2: Definition of RS-232 interface.

Pin	Interface name	Function Definition
1	CD	Carrier detective
2	RXD	Receive data
3	TXD	Send data
4	DTR	Data terminal ready
5	GND	Grounding
6	DSR	Data ready
7	RTS	Request to send
8	CTS	Clear the send
9	RI	Ringing indication

The commonly used configuration for RS-232 communication is eight data bits, no parity bit, and one stop bit. As shown in Figure 4, a complete byte includes a start bit, 8 data bits, and a stop bit. The transmission module requires eleven baud rate clock pulses to complete the transmission of one data set, while the RS-232 receiver samples at the midpoint of each data bit.

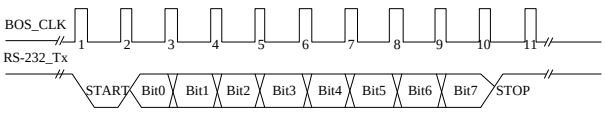

Figure 4: Data transmission timing logic of the RS-232 interface.

The interface receive and transmit module design is shown in Figure 5.

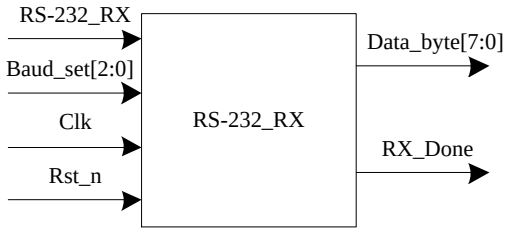

(a) Receiving module

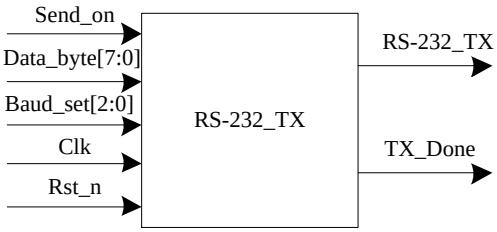

(b) Transmitting module

Figure 5: Design of RS-232 interface module.

When sending data, first encapsulate the fault detection results of uneven tracks, and then send them byte by byte according to the RS-232 protocol. The sending module generates a clock signal to control the speed according to the preset baud rate. After STM32F103ZET6 is ready, it sends the command. The module receives the command and sends it, monitoring the status in real time. If there is an error, it will provide feedback. When receiving, the RS-232 terminal samples at the midpoint of the data, parses it in the same format, and cooperates with the microprocessor to detect the starting identifier before receiving. During the process, it provides feedback on the receiving status.

After transmitting the fault data via wired communication, the microcontroller processes the signals for fault detection using the JADE algorithm.

2.5 Railway irregularity fault detection based on the jade algorithm

The microcontroller plays a central role in the entire railway track unevenness detection system [15], serving as the core for data processing, analysis, command transmission, and other key operations. The STM32F103ZET6 is selected as the main chip for the railway track unevenness detection system. When the microcontroller STM32F103ZET6 receives vibration signals from the ADXL345, it processes and analyzes these signals using a JADE-based blind source separation method to achieve fault detection of railway track unevenness.

To achieve real-time operation of JADE algorithm on STM32F103ZET6 microprocessor, the following key optimization measures are taken in this study:

(1) Simplified computational load: Using frame processing mode to segment continuous signals for processing. At the same time, channel fusion is used to reduce the dimensionality of three-axis sensor data, reducing the observation signal from 3D to 2D and significantly reducing the complexity of subsequent matrix operations.

(2) Algorithm and computational optimization: Due to the lack of FPU in the Cortex-M3 core, all floating-point operations are converted to fixed-point operations and accelerated using the CMSIS-DSP library. For this purpose, a lookup table is used instead of real-time computation for complex functions. Set a maximum iteration limit for the JAD iteration process to ensure controllable worst-case execution time.

(3) Resource management and performance: Adopting static memory allocation to avoid the uncertainty of dynamic allocation, ensuring that the total memory usage is controlled within 20 KB. According to actual testing, at a frequency of 72 MHz, the average processing time for a single frame of data is about 65 ms, which meets the real-time requirement of the system $\leqslant$ 90 ms.

Simple spectral analysis alone cannot separate individual vibration sources [16], and the processed spectrum is the result of a mixture of multiple vibration signals. When there are strong harmonic components at certain frequencies, they can affect nearby harmonic components in the power spectrum, leading to spectral aliasing. Blind source separation algorithms can separate multiple source vibration signals for individual analysis, reduce mutual interference among different source signals, improve the accuracy of vibration signal separation, and lay the foundation for the separation and extraction of fault information. To some extent, they also reduce the difficulty of extracting track fault features. Additionally, since each track segment has the same length, when faults occur in the track region, the resulting fault vibrations are periodic, which is distinctly different from general aperiodic vibration signals. Blind source separation algorithms are particularly suitable for separating periodic fault vibration signals [17].

The mathematical model of the blind source separation algorithm can be expressed as:

$$x(t) = As(t) + z(t) \tag{1}$$

Where, A represents the mixing matrix, describing the mixing process when multiple source vibration signals are input into the system; $x(t)$ indicates the M -dimensional observation vector obtained from M ADXL345 vibration accelerometers, i.e., the mixed vibration signals:

$$x(t) = [x_1(t), x_2(t), ..., x_m(t)]^T \tag{2}$$

Where, $s(t)$ represents N independent source track vibration signals, which need to be separated and identified:

$$s(t) = [s_1(t), s_2(t), ..., s_n(t)]^T \tag{3}$$

Where, $z(t)$ represents M -dimensional noise signal, i.e.:

$$z(t) = [z_1(t), z_2(t), ..., z_m(t)]^T \tag{4}$$

When using the blind source separation method to analyze the track vibration signal problem, it can be described as follows: In a multi - input multi - output train wheel - rail coupling system, for the collected

vibration signal $x(t)$, an inverse system is sought to reconstruct the source vibration signal $s(t)$ [18]. That is, through the known observation signal $x(t)$, a separation matrix E is found, so that $y = Ex(t) = s(t)$, where y is the estimated source vibration signal after separation. The basic principle of blind source separation lies in the mixing matrix A when multiple source vibration signals are input into the system. The mixed vibration signal is detected by multiple ADXL345 vibration acceleration sensors to obtain the detection signal $x(t)$. Performing blind source separation on the detection signal $x(t)$ is to start from the detection signal, and then find the blind separation matrix E, perform blind separation on the detection signal, and find the track fault information contained in the separation result.

Vibration signals are an important information source for track fault feature recognition [19]. Fault detection is carried out through vibration signals. Since the vibration signal data collected by the ADXL345 vibration acceleration sensor is often a mixture of several signals, using traditional filtering methods will filter out some useful feature information while filtering out noise. The JADE algorithm is an important part of the blind source separation algorithm, also called the feature matrix approximate joint diagonalization blind separation algorithm based on fourth - order cumulants [20]. This algorithm has very high separation performance, and its separation performance has nothing to do with the mixing matrix. It can find the source information signal only by relying on the detection signal when the mixing mode of the input information is not understood and there is little or no prior information. The definition of the fourth - order cumulant matrix is as follows:

$$F_{ij}(B) = \sum_{h=1}^{N}\sum_{l=1}^{N} K_{ijhl}(\hat{x}) b_{hl} \tag{5}$$

Where, B represents an arbitrary $N \times N$ -order matrix; F_{ij} denotes a matrix obtained through a linear transformation in the $N \times N$ space; b_{hl} indicates the element in the h -th row and l -th column of matrix B ; the mixed vibration signal x after whitening processing results in $\hat{x}$; $K_{ijhl}(\hat{x})$ represents a linear combination of the fourth-order accumulated quantities of the four components i , j , h and l .

The product of the whitening matrix Q and the mixing matrix A is defined as matrix O:

$$O = QA \tag{6}$$

Where $O = [o_1, o_2, ..., o_m, o_N]$, $o_m = [o_{m1}, o_{m2}, ..., o_{mN}]^T$, $m = 1, 2, ..., N$.

If the matrix B is chosen to satisfy $B = o_m o_m^T$, then the fourth-order cumulant matrix can be expressed as:

$$F_{ij}(B) = \sum_{q=1}^{N} o_{mh} o_{ml} cum(\hat{x}_i, \hat{x}_j, x_h, x_l) \tag{7}$$

Because the track vibration source signals are independent, when $q = m$, the corresponding cumulants have non-zero values. In this case, the fourth-order cumulant can be expressed as:

$$\begin{aligned} F_{ij}(B) &= \sum_{q=1}^{N} o_{qi} o_{qj} \delta_{mq} \delta_{mq} k_4(s_q) \\ &= o_{mi} o_{mj} k_4(s_m) = b_{ij} k_4(s_m) \end{aligned} \tag{8}$$

At this point, the matrix B is the eigenmatrix of $F(B)$, and the fourth-order cumulant of the source vibration signal is the eigenvalue of the eigenmatrix. Performing eigenvalue decomposition on the matrix, the eigenmatrix corresponds one-to-one with the eigenvalues. Each source vibration signal has a different fourth-order cumulant, and its corresponding eigenmatrix B is also different, which in turn makes o_m different. The mixed matrix A can be represented by the matrix O composed of o_m .

$$A = Q^{-1}QA = Q^{-1}O \tag{9}$$

Performing inverse operation on the mixed matrix A to obtain the separation of source vibration signals, $s' = A^{-1}\hat{x}$, can be achieved when all eigenvalues of the fourth-order cumulant matrix $F(B)$ are distinct. If the eigenvalues are not all different, separation cannot be performed. The JADE algorithm solves this problem. Because $F(B)$ is a symmetric matrix, $B = o_m o_m^T$ is its eigenmatrix, and $F(B)$ can be expressed in the form of $O\Lambda(B)O^T$.

$$\Lambda(B) = diag(k_4(s_1) o_1 B o_1^T, ..., k_4(s_N) o_N B o_N^T) \tag{10}$$

Transform matrix O applied to $F(B)$ to obtain a diagonal matrix, utilizing the diagonalization property to find matrix O . Define an objective function:

$$J_{JADE}(O) = \sum_{i=1}^{K} \left\| diag(O^T F(B_i) O) \right\|^2 \tag{11}$$

Where, $\left\| diag(O^T F(B_i) O) \right\|^2$ represents the sum of squares of the diagonal elements of the diagonal matrix $\Lambda(B)$. This value is invariant during diagonalization. Maximizing the objective function allows us to find the ideal matrix O , thereby enabling the separation of source vibration signals. The estimated separation matrix is $E = O^T Q$, and thus the estimated source signal is $y(t) = Ex(t)$.

In summary, by applying the JADE algorithm to the mixed vibration signals collected by the ADXL345 vibration accelerometer, it is possible to effectively separate each source vibration signal, extract useful fault feature information, and achieve accurate detection of railway track irregularities.

The pseudocode of JADE algorithm is as follows:

```
# Pseudo-code: JADE Integration in Track Vibration Signal Processing
import numpy as np
from scipy import linalg
```

```
# Step 1: Read and preprocess data
raw_signal = read_vibration_data()  # Read raw vibration data from sensor
x_normalized = (raw_signal - np.mean(raw_signal, axis=0)) / np.std(raw_signal, axis=0)  # Normalize

# Step 2: Execute JADE Blind Source Separation
# 2.1 Whiten the normalized observed signal x_normalized
x_whitened, whitening_matrix = whiten(x_normalized)

# 2.2 Compute fourth-order cumulant matrices of the whitened signal
cumulant_matrices = compute_fourth_order_cumulants(x_whitened)

# 2.3 Joint Approximate Diagonalization (JADE Core)
# Find a unitary matrix U that diagonalizes U^T * CumulantMatrix_i * U
U = joint_approximate_diagonalization(cumulant_matrices)

# 2.4 Estimate separating matrix and obtain source signals
separating_matrix = U.T @ whitening_matrix
estimated_sources = separating_matrix @ x_normalized.T  # Separated independent sources

# Step 3: Feature Extraction and Fault Classification (Based on separated sources)
features = extract_features(estimated_sources)  # Extract time-frequency features
fault_type, fault_location = classifier.predict(features)  # Classify for fault diagnosis

# Step 4: Output Results
output_result(fault_type, fault_location, severity)
```

In addition, as mentioned earlier, the core premise of blind source separation algorithm based on JADE is to assume that the source signals are statistically independent of each other. In the context of railway track vibration applications, this assumption has its physical validity. The complex vibration signals generated by the wheel rail system during train operation can be regarded as a linear mixture of multiple physically independent vibration sources. These potential independent sources include:

(1) Periodic vibrations induced by geometric irregularities such as uneven height and orientation of the track.

(2) Transient impact vibration caused by rail welds, corrugation, or locally isolated defects such as peeling and cracking.

(3) The inherent mechanical vibration of components such as vehicle bogies and wheels.

(4) Background noise from the environment and measurement system.

The generation mechanism and transmission path of these vibration sources are physically different, and the correlation in statistical characteristics is weak. Therefore, it is reasonable to consider them as statistically independent source signals.

Although a complex single defect may indeed generate correlated vibration responses in multiple directions of space. In this case, the vibration component generated by the defect may not strictly satisfy statistical independence. However, the advantage of the JADE algorithm lies in its commitment to finding a linear transformation that maximizes the statistical independence of the output signal. Even if there is weak correlation or partial correlation in the source signal, this algorithm can still effectively achieve approximate blind separation of the signal. Although the separated signal may not be a completely "pure" physical source, its main energy is usually concentrated in different fault characteristic modes, greatly reducing the degree of signal aliasing and making the characteristic components related to specific track irregularities more prominent in both time and frequency domains. This separation effect lays a solid foundation for accurately extracting fault features in the future.

3 Experimental analysis

3.1 Experimental preparation

To verify the effectiveness of the proposed method for railway track irregularity fault detection, an actual operational railway line was selected as the experimental subject. This line includes various track types, such as standard steel rails and seamless rails, as well as different sections, such as straight segments, curves, and turnout areas, to ensure the comprehensiveness and representativeness of the experimental results. The total length of the test section is 30 kilometers, with 8 key monitoring points installed, each equipped with a railway track irregularity online fault detection system based on the aforementioned design. At each monitoring point, ADXL345 vibration acceleration sensors were installed according to the design requirements, ensuring close contact with the track. The installation positions follow the principles of high stiffness, minimal structural damping, and proximity to vibration sources, as shown in Figure 6.

Figure 6: Installation position of the ADXL345 vibration acceleration sensor.

The main performance parameters of the ADXL345 vibration acceleration sensors are listed in Table 3. The hardware connection and debugging of the lower computer system (including the STM32F103ZET6 microcontroller, power module, etc.) were completed to ensure proper communication between modules. The upper computer and lower computer are connected via RS-232 to USB interface, and the upper computer software was installed and configured to receive and display fault detection result data.

Table 3: Main performance parameters of ADXL345 vibration acceleration sensor.

Parameters	Test conditions	Maximum value	Minimum value	Standard value	Unit
Sensitivity	All g ranges, full resolution	3.9	3.5	-	mg/LSB
Measurement range	Optional for users	-	-	±2, ±4, ±8, ±16	g
Noise along the X and Y axes	2g, 10-bit resolution or all g ranges, full resolution,ODR=100Hz	-	-	0.75	LSB rms
Z-axis noise	2g, 10-bit resolution or all g ranges, full resolution,ODR=100Hz	-	-	1.1	LSB rms
Bandwidth	Optional for users	3200	0.1	-	HZ

In order to quantitatively analyze the specific impact of sensor installation location on fault detection accuracy, this study selected three representative different installation locations near the same monitoring point for comparative experiments:

(1) Position A (optimal position): Strictly following the installation principles in Section 2.2, located in the rail waist area, this position has high stiffness, low structural damping, and is adjacent to the wheel rail force transmission path.

(2) Position B (suboptimal position): Installed on the upper surface of the rail bottom, although the stiffness is still acceptable, it is relatively far away from the main vibration source (rail head), and the vibration signal will experience attenuation and distortion during transmission.

(3) Position C (poor position): Installed on the rail sleeper or in contact with the ballast at the bottom edge of the track, this position has high structural damping and is susceptible to interference from non track geometric irregularities such as track bed vibration.

When the train passes at a speed of 60 km/h, the same system is used to collect vibration data from three different positions and perform fault detection. The results are compared with the "ground truth value", and it is found that the installation position of the sensor has a decisive impact on the detection accuracy of the system. Compared with the optimal position A, the positioning error of the suboptimal position B increased by 94%, and the recognition accuracy decreased by 11.5 percentage points. This is because the high-frequency components of the vibration signal attenuate more severely during the transmission from the rail head to the rail bottom, resulting in blurred fault characteristics. At the poor position C, the performance deteriorates sharply, the positioning error increases to 300%, and the recognition accuracy drops significantly to 65%. The reason is that a large amount of non orbital geometric vibration noise is mixed in the signals collected at this location, which seriously undermines the basic assumption of "source signal statistical independence" in the JADE algorithm, leading to the failure of blind source separation and the inability to effectively extract feature components related to track irregularities. Therefore, in order to ensure optimal detection performance of this system, sensors must be installed at positions with high track stiffness, low structural damping, and as close as possible to the wheel rail contact point to avoid signal attenuation and external interference, thereby ensuring accurate separation of fault characteristics reflecting the true state of the track from mixed vibration signals.

After completing the hardware connection and debugging of the lower computer system, special tests were conducted on its key performance to evaluate the reliability of its power module in complex railway environments. According to testing, it is known that:

(1) Within the fluctuation range of 12-24V DC input voltage, the 5V voltage ripple output by MP2359 is less than 50mV, and the 3.3V voltage deviation output by AM11117 is less than 1%, providing a stable working foundation for the system.

(2) The polarity reversal protection test shows that the designed anti reverse diode can effectively withstand a reverse current of 5A without any device damage or system abnormalities.

(3) Under a continuous 48 hour full load operation test at an ambient temperature of 25℃, the shell temperatures of MP2359 and AM11117 chips remained stable below 65℃ and 55℃, respectively, far below their maximum junction temperature.

This result fully demonstrates that the dual level power management scheme has good thermal stability and long-term operational reliability, meeting the demanding requirements of railway field applications.

3.2 Ablation verification

In order to evaluate the effectiveness of the JADE algorithm in blind source separation, ablation

experiments were first conducted to compare JADE with two common BSS methods (FastICA and SOBI). FastICA is based on maximizing negative entropy and is suitable for separating non-Gaussian signals, but may have a slower convergence speed; SOBI is based on second-order statistics for joint diagonalization, which is suitable for time-dependent signals, but has limited ability to separate non-Gaussian signals. The experiment used the same track vibration dataset (sampling frequency of 10240 Hz, train speeds of 60 km/h and 80 km/h), and applied these three methods for signal separation, comparing their separation performance and accuracy. The results are shown in Table 4.

Table 4: Ablation study results comparing the separation performance and accuracy of different BSS methods.

BSS methods	Operating speed (km/h)	Separation performance indicators (signal-to-noise ratio/dB)	Accuracy index (fault type recognition accuracy/%)
JADE	60	18.5	1.8
	80	17.1	2.2
FastICA	60	16.2	2.5
	80	14.8	2.8
SOBI	60	14.0	3.0
	80	12.5	3.5

From Table 4, it can be seen that the JADE algorithm significantly outperforms FastICA and SOBI in terms of signal-to-noise ratio. This indicates that JADE's method based on fourth-order cumulants can more effectively extract independent components related to non Gaussian fault impact signals from mixed vibration signals, while better preserving the waveform characteristics of the original fault signals. Better separation performance directly translates into higher fault detection accuracy. The JADE method achieved lower accuracy in identifying fault types under all speed conditions. This is due to its excellent signal decoupling ability, which makes subsequent feature extraction and fault recognition more reliable.

This ablation experiment proves that in the blind source separation task of railway track vibration signals faced by this system, the JADE algorithm is the optimal choice in terms of separation performance and final fault detection accuracy due to its efficient processing ability for non Gaussian source signals.

3.3 Basic inspection

The train conducted multiple round-trip runs on the test section at normal operating speeds (60–80 km/h). During each run, the lower-level system continuously collected track vibration signals in real time. The data sampling frequency was 10,240 Hz, with continuous sampling for 26 seconds, resulting in a total of 231,234 data points. The selection of the sampling rate (10240 Hz) strictly follows the Nyquist sampling theorem and is based on the characteristics of railway track vibration signals. The main vibration frequency components excited by track irregularities are usually distributed between 0-2000 Hz, but their higher-order harmonics and transient shock components can extend to 4000-5000 Hz. To ensure the capture of these key high-frequency fault features without aliasing, the sampling rate must be higher than twice the highest effective frequency. The sampling rate of 10240 Hz provides sufficient margin for this and can fully preserve the signal spectrum information. This setting also conforms to common practices in the field of railway vibration detection, balancing hardware processing capabilities and data volume while ensuring signal fidelity.

Before inputting the raw data into the JADE algorithm, this study set up the following preprocessing process: after performing zero mean and variance normalization on the observed signals of each channel, a first-order high pass filter was used to eliminate the linear trend term caused by sensor temperature drift or slow environmental changes in the signal.

In this study, 'Ground Truth Fault' refers to track geometric irregularities that exceed maintenance thresholds and are confirmed through high-precision independent measurement methods. By jointly using high-precision track inspection vehicles and total station geodetic surveying, a millimeter level precision "ground truth" dataset of track geometry parameters for the experimental section is obtained. Then, using GPS timestamps and odometer information, the vibration data collected by this system is accurately aligned with the "ground truth" data in terms of time and space. Finally, write a script program to automatically scan the "ground truth" data, identify all geometric deviation positions and types that exceed the preset threshold, and label the vibration data segments within a specific time window before and after these positions with corresponding fault type labels. These labels serve as benchmarks for evaluating the accuracy of subsequent algorithm recognition.

The time-domain record curves of the vibration information at three randomly selected monitoring points are shown in Figure 7.

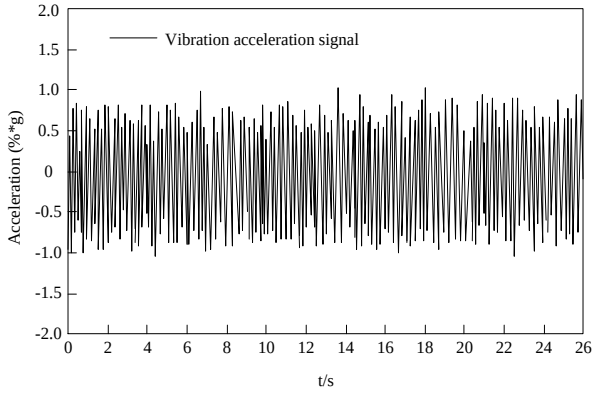

(a) Monitoring Point a

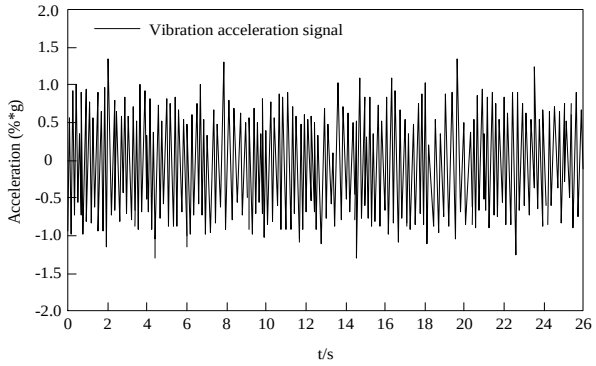

(b) Monitoring Point b

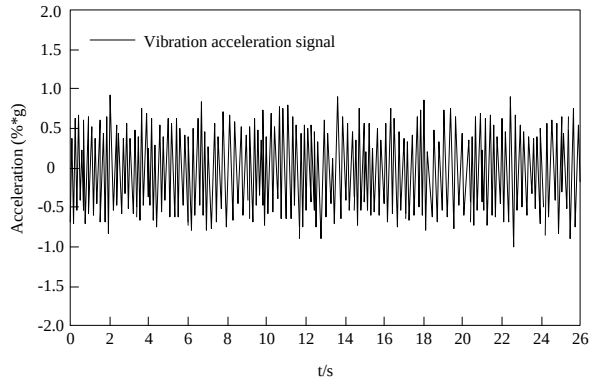

(c) Monitoring Point c

Figure 7: Acquisition results of vibration signals.

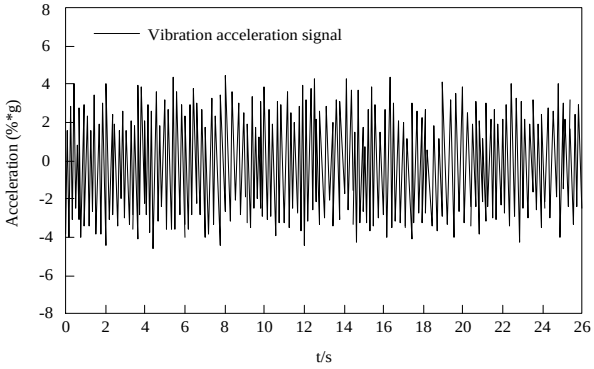

(a) Monitoring Point a

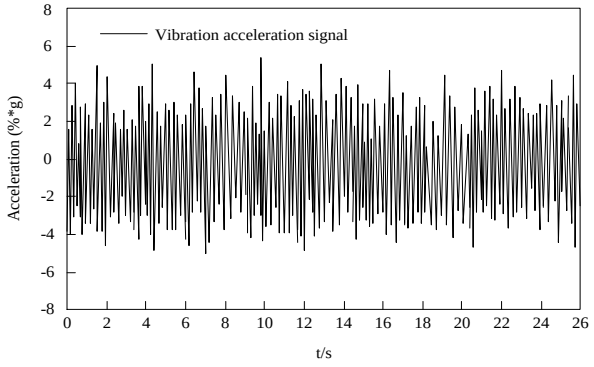

(b) Monitoring Point b

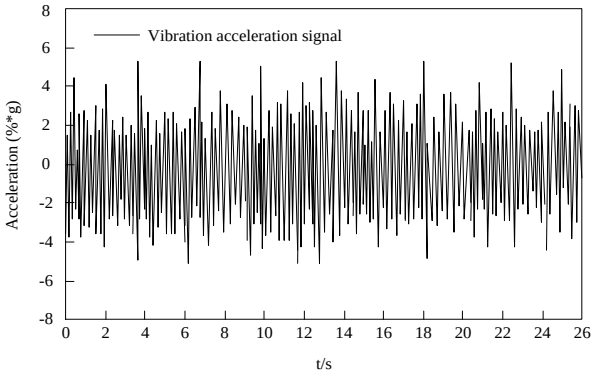

(c) Monitoring Point c

Figure 8: shows the time-domain graphs of each monitored vibration signal after separation.

As shown in Figure 7, the vibration signals at the three monitoring points all contain fault information related to track irregularities. Observing the time-domain signals, it is evident that the irregularity fault information is mixed and lacks clear features, necessitating further data processing and analysis.

The collected track vibration signals are transmitted via IIC bus to the STM32F103ZET6 microcontroller. After preprocessing the acquired vibration signals, the proposed method is used to separate the signals, making each source signal independent. The components related to track irregularities are extracted, as shown in Figure 8.

As demonstrated in Figure 8, after completing the signal separation operation, the vibration signals at each monitoring point accurately exhibit the characteristic of periodic variation induced by track irregularities. Comparing Figure 8 with the time-domain waveform of the original vibration signals in Figure 7, it is evident that the features of each component of the original vibration signals in the time domain are blurred and difficult to identify accurately. After signal separation processing, the aliasing between the independent components of the vibration signals at each monitoring point is significantly reduced, and the vibration signal components related to track irregularities become clearer in the time domain. This change makes it possible to detect track irregularity faults based on these signals and can achieve relatively ideal detection results.

To further verify the performance of the proposed railway track irregularity online fault detection system, comparative experiments were conducted using the HybridGAN method, data mining methods, and the method proposed in this paper. Under the same experimental track segment and conditions, the three methods were used to detect track irregularity faults at different train speeds.

3.4 Comparative inspection

To ensure the accuracy and credibility of experimental results, it is necessary to establish high-precision benchmark references (i.e. "ground truth") for the location, type, and severity of track irregularities. This study used the following two methods to collaboratively establish the benchmark:

(1) High precision track geometry inspection vehicle measurement: Before and after the operation of the experimental train, a high-precision track geometry inspection vehicle equipped with inertial reference method and laser camera technology was used to conduct multiple surveys of the entire 30-kilometer experimental section. This inspection vehicle is capable of accurately measuring and recording the absolute geometric parameters of the track, including height, track orientation, horizontal, triangular pits, and track gauge, generating detailed geometric state reference maps of the track. This benchmark map serves as the primary basis for verifying the positioning accuracy of this system.

(2) Verification of total station manual geodetic survey: For all suspected fault points detected by the system and reported by the inspection vehicle, a high-precision total station (Leica TS60, angle accuracy 0.5", distance measurement accuracy 0.6 mm+1 ppm) is further used for manual geodetic survey under static conditions. Accurately measure the three-dimensional coordinates of key control points on the track at intervals of 0.5 meters within a range of 10 meters before and after the fault point, in order to obtain the "true value" of the fault location and geometric deviation, which is used for the final confirmation and calibration of millimeter level positioning information of the fault.

After outputting the fault location, type, and roughness value, it is first automatically compared with the reference map generated by the track geometry inspection vehicle. Subsequently, for all successfully compared fault points, their positioning errors were calculated by comparing the "true value" coordinates measured by the total station with the mileage and relative position reported by the system. The accuracy of identifying fault types is ultimately confirmed and classified by on-site engineering and technical personnel based on inspection vehicle reports, total station data, and on-site investigations.

The HybridGAN method and data mining method were replicated and compared in the same experimental section and train schedule. The specific implementation details of both are as follows:

When applying the HybridGAN method for parallel image data acquisition, an industrial grade linear array camera system (model Basler raL2048-48gm) is installed at key positions on the front and bottom of the test train, in conjunction with a high brightness linear LED light source, to ensure clear capture of the surface image of the track at the train's operating speed. The camera is connected to the onboard industrial computer through a gigabit Ethernet interface, and the image acquisition frequency matches the train speed and spatial resolution, ensuring coverage of the entire experimental section. The model is trained using the Adam optimizer, with an initial learning rate of 1 ×10-4 and a batch size of 8. The image input resolution is uniformly adjusted to 512x512 pixels. Input real-time captured images into HybridGAN for quality enhancement, and then use a pre trained YOLOv5 object detection network on the same dataset to identify and locate orbit defects from the enhanced images.

When applying data mining methods, a large amount of historical vibration data containing labels collected by the lower computer in the same experimental section at different times is used as the basic dataset, and the ACO algorithm is used for feature selection. The population size of ACO is set to 100, the number of iterations is 200, the pheromone heuristic factor is 1.0, and the expected heuristic factor is 5.0. Extract a total of 35 initial features from the time and frequency domains of vibration signals, and ACO selects 15 key feature combinations that are most relevant to high impact loads. Then, based on the features selected by ACO, a classification model is constructed using the LAD method. Finally, generate a combined classifier based on these patterns for fault type determination of real-time collected vibration signal data.

The fault detection results of the three methods are shown in Table 5.

Table 5: Test results of different methods.

Operating speed (km/h)	Detection method	Positioning error (mm)	Fault type identification accuracy (%)	Standard deviation of fault type identification accuracy (%)	Detection time (ms)	Recall rate (%)
60	HybridGAN method	3.2	72	±4.5	120	68
	Data mining method	4.0	68	±5.2	150	65
	Method of this article	1.8	96	±1.2	90	94
70	HybridGAN method	3.5	70	±4.8	130	66
	Data mining method	4.3	65	±5.5	160	62
	Method of this article	2	92	±1.5	93	90
80	HybridGAN method	3.8	68	±5.0	140	64

	Data mining method	4.6	62	±5.8	170	58
	Method of this article	2.2	90	±1.8	95	88
Operating speed (km/h)	Detection method	F1 score	False positive rate (%)	False negative rate (%)	Accuracy (%)	Macro average AUC
60	HybridGAN method	70.0	12	20	70.2	0.72
	Data mining method	66.5	18	27	96.5	0.98
	Method of this article	95.0	3	4	72.0	0.76
70	HybridGAN method	68.0	14	24	67.8	0.70
	Data mining method	63.5	20	33	93.2	0.96
	Method of this article	91.0	4	6	70.5	0.74
80	HybridGAN method	66.0	16	28	65.0	0.68
	Data mining method	60.0	24	40	91.0	0.94
	Method of this article	89.0	5	7	70.2	0.72

As shown in Table 5, it can be seen that the method of this article outperforms the HybridGAN method and data mining method in the speed range of 60-80 km/h. In terms of positioning accuracy, the average error of the method of this article at different speeds is only 1.8-2.2 mm, far lower than the 3.2-3.8 mm of the HybridGAN method and the 4.0-4.6 mm of the data mining method; In terms of fault recognition accuracy, the method of this article achieves 90%-96%, significantly higher than the other two methods' 62%-72%, demonstrating stronger feature extraction and classification capabilities. Meanwhile, the method of this article also has significant advantages in real-time detection, with an average detection time controlled between 90-95 ms, which is about 30% and 45% higher than HybridGAN and data mining methods, respectively, better meeting the real-time requirements of online monitoring. In terms of comprehensive performance indicators, the F1 score of method of this article is as high as 89%-95%, the recall rate is maintained at 88%-94%, and the false positive and false negative rates are both controlled at a low level ($\leqslant$ 7%), indicating that the system effectively suppresses false positives and false negatives while identifying real faults. In addition, the standard deviation of the recognition accuracy of the method of this article at different speeds is only 1.2% -1.8%, demonstrating good stability and adaptability.

In summary, the method of this article not only leads comprehensively in key performance indicators, but also achieves a good balance between accuracy, speed, and reliability, providing an effective solution for real-time monitoring of track status in complex railway environments.

4 Discussion

To clearly demonstrate the differences between this method and existing technologies, a comprehensive analysis of the core characteristics of the two comparative methods is presented in Table 6.

Table 6: Comparative analysis of existing methods.

Method	HybridGAN method	Data mining method
Input modality	Orbital image	Vibration signal
Feature extraction method	GAN enhances image quality, combined with object detection network	Ant Colony Optimization (ACO) selects features and Logical Data Analysis (LAD) constructs patterns
Accuracy	72%	68%
Main limitations	Dependent on lighting and weather conditions; Unable to detect non surface defects such as track geometry deformation; Image processing incurs high computational costs.	Relying on a large amount of high-quality historical data; Sensitive to data noise; The extracted features have unclear physical meanings and weak generalization ability.

The limitation of traditional track fault detection methods, such as HybridGAN, is that they can only infer from surface visual information and lack direct perception of the internal vibration mechanism and dynamic mechanics of the track structure. Therefore, they cannot effectively detect key geometric irregularities such as height and track orientation. Although data mining methods directly process vibration signals, they rely on a "black box" search for statistical feature patterns from historical data. The extracted features have weak correlation with specific physical fault mechanisms, and their performance is easily constrained by data quality and completeness.

The core advantage of this method lies in its direct targeting of the physical essence of orbital vibration. Through the JADE blind source separation algorithm, the system can directly decouple physically and statistically independent vibration source components from the mixed observation signals, which closely correspond to specific physical phenomena such as periodic irregularities and local impacts in the orbit. This method does not rely on massive labeled historical data, but on reasonable assumptions about the mechanism of

vibration signal generation and advanced signal processing techniques, thus achieving high-precision and robust online detection and localization of track roughness faults, solving the inherent shortcomings of traditional methods in physical interpretability, environmental adaptability, and data dependence.

The key to the excellent performance of the JADE algorithm in this system is its ability to effectively separate source signals with non-Gaussian distributions by utilizing the high-order statistical properties (fourth-order cumulants) of the signal. Under the background of track vibration, the periodic impact signal caused by unevenness precisely conforms to this characteristic, enabling JADE to extract fault components more accurately than traditional methods that rely solely on second-order statistics or shallow features. However, the cost of its outstanding performance is high computational complexity. This design achieves a good balance between computing power and real-time requirements (detection time $\leqslant$ 90ms) by selecting STM32F103ZET6 microprocessor with FPU and optimizing matrix operations. The experiment shows that the system performance slightly decreases with the increase of train speed. The increase in speed causes the main frequency of vibration to shift upward, background noise to increase, and may lead to more complex modal coupling, which exacerbates the difficulty of signal separation and is the main reason for the increase in positioning error and the slight decrease in recognition accuracy. However, the JADE algorithm is insensitive to common Gaussian noise and exhibits a certain level of inherent robustness. At the same time, the system exhibits stable detection capability in both straight and curved segments, with the key being that the source signal separated by the algorithm is directly related to the inherent geometric features of the track (such as the periodic lateral shift of the curve), proving that this method has good adaptability to different track structures.

The railway track roughness online fault detection system based on vibration mechanism characteristics proposed in this study exhibits good detection performance in the speed range of 60-80 km/h. However, with the significant increase in train operating speed, the system may face a series of new challenges. Firstly, high-speed operation introduces vibration components with wider frequency bands and higher energy, leading to increased signal aliasing, which may exceed the separation capability of the current JADE algorithm and affect the accuracy of fault feature extraction. Secondly, the matching between the dynamic response characteristics of sensors and the sampling frequency under high-frequency impact, as well as the real-time requirements for data transmission, will place higher demands on the hardware system. In addition, the wheel rail coupling vibration under high-speed conditions is more complex, and the effects of environmental noise and vehicle vibration are also more significant, which may reduce the rationality of the assumption of "source signal independence" in blind source separation.

To address the above challenges, future research work can be carried out from the following aspects: firstly, optimizing blind source separation algorithms, introducing adaptive or deep learning assisted signal processing strategies, and improving the feature decoupling ability of high-speed vibration signals; The second is to consider integrating multimodal sensor data, such as introducing gyroscopes or inertial measurement units, to obtain dynamic changes in the spatial attitude of the orbit, thereby further improving the accuracy of fault identification and localization based on multidimensional information fusion; The third is to enhance the edge computing capability of the system, and meet the strict requirements for data processing speed and stability in high-speed scenarios through more powerful processors and optimized real-time operating systems.

In the future, through the above improvements, it is expected to expand the applicability of this system to railway lines with higher speed levels, further enhancing its reliability and practicality in complex operating environments.

5 Conclusion

Online detection of railway track irregularities via jade-based blind source separation and MEMS accelerometry in this paper demonstrates good performance and practicality. Experimental validation shows that the system can effectively process the mixed vibration signals collected by the ADXL345 sensor, separate the vibration components related to track unevenness, reduce the aliasing among independent components, and produce clear time-domain features, laying a foundation for fault detection. Compared with the HybridGAN method and data mining methods, under different train speeds, our method achieves smaller positioning errors, higher fault type recognition accuracy, and shorter detection times, enabling more precise fault localization, accurate fault type judgment, and faster fault discovery. Additionally, the upper computer can visually display information such as the type, location, and degree of track unevenness, with search functionality, easy operation, and the system is equipped with dual-level power management and reverse connection protection to ensure stable and reliable operation in complex railway environments. In summary, this system can effectively improve the efficiency and quality of railway track maintenance, ensure the safety and stability of railway transportation, and has high application value and prospects for promotion.

Acknowledgment

This study was supported by 2024 Science and Technology Research Projects in Henan Province; Research and Application of Railway Track Irregularity Online Fault Detection System Based on Vibration Mechanism Characteristics (242102240130) and Key Research Project of Universities in Henan Province in 2025, Research and Application of Key Technologies for

High-Speed Rail Track Online Fault Detection System Based on Transfer Learning (25A580011).

References

[1] González-Carbajal J., Urda, P., Muoz, S., & José L. Escalona. (2024). Estimation of the trajectory and attitude of railway vehicles using inertial sensors with application to track geometry measurement. Vehicle System Dynamics, 62(4), 837-863. https://doi.org/10.1080/00423114.2023.2203865

[2] Salcher, P., Adam, C., & Knig, P. (2022). A probabilistic model for the amplification of the vibration response of railway bridges due to random track unevenness in high-speed traffic. International Journal of Structural Stability and Dynamics, 220(10), 2241009. https://doi.org/10.1142/S0219455422410097

[3] Gupta, R. K., & Sowmiya Chawla, A. M. A. (2022). Performance evaluation of micropiles as a ground improvement technique for existing railway tracks: finite-element and genetic programming approach. International Journal of Geomechanics, 22(3), 4021287. https://doi.org/10.1061/(ASCE)GM.1943-5622.0002270

[4] Cheng, M. Y., Khasani, R. R., & Setiono, K. (2023). Image quality enhancement using hybridgan for automated railway track defect recognition. Automation in Construction, 146, 104669. https://doi.org/10.1016/j.autcon.2022.104669

[5] Yang, J., Stewart, E., & Entezami, M. (2022). Decomposition methods for impact-based fault detection algorithms in railway inspection applications. IET Signal Process, 16, 935-944. https://doi.org/10.1049/sil2.12093

[6] Hany, O., & Soumaya, Y. (2023). Condition-based monitoring of the rail wheel using logical analysis of data and ant colony optimization. Journal of Quality in Maintenance Engineering, 29(2), 377-400. https://doi.org/10.1108/JQME-01-2022-0004

[7] Koohmishi, M., Kaewunruen, S., Chang, L., & Guo, Y. (2024). Advancing railway track health monitoring: integrating gpr, insar and machine learning for enhanced asset management. Automation in Construction, 162, 105378. https://doi.org/10.1016/j.autcon.2024.105378

[8] Bayat, M., Pakar, I., Ziehl, P. (2021). Nonlinear vibration of axially loaded railway track systems using analytical approach. Journal of Low Frequency Noise, Vibration and Active Control, 40(4), 1896-1906. https://doi.org/10.1177/14613484211004190

[9] Tran, L. H., Do, T. T. H., & Le-Nguyen, K. (2023). Influence of beam models on dynamic responses of ballasted railway track subjected to moving loads. Archive of Applied Mechanics, 93, 3665-3682. https://doi.org/10.1007/s00419-023-02459-4

[10] Luccidi, Y., Rezende, A. B., & Fonseca, T. M. P. R. (2022). Study of the running-in period in the twin-disc wear test using steel from a class c forged railway wheel. Journal of Tribology, 144(11),114501. https://doi.org/10.1115/1.4054758

[11] Jin, J., Kim, H., Koh, H. I., & Park, J. (2022). Railway noise reduction by periodic tuned particle impact damper with bounce and pitch-coupled vibration modes. Composite Structures, 284(3), 115230. https://doi.org/10.1016/j.compstruct.2022.115230

[12] Koc, W. (2022). Estimation of the horizontal curvature of the railway track axis with the use of a moving chord based on geodetic measurements. Journal of Surveying Engineering, 148(4), 04022007. https://doi.org/10.1061/(ASCE)SU.1943-5428.0000402

[13] Dash, S. K. (2022). Closure to "geogrid reinforcement for stiffness improvement of railway track formation over clay subgrade" by sujit kumar dash and anjan majee. International Journal of Geomechanics, 22(10), 07022011. https://doi.org/10.1061/(ASCE)GM.1943-5622.0002577

[14] Babaahmadi-Fooladi, A., Sadeghkhani, I., & Mehrizi-Sani, A. (2023). A current wave-shape based feeder protection for dc electric railway traction systems. Electric Power Systems Research, 225, 109817. https://doi.org/10.1016/j.epsr.2023.109817

[15] Konyakhin, I., Han, X., Renpu, L., Jiawen, Y., Guifu, H., & Xin, T. (2022). Optic-electronics stereo system for spatial position measurement of railway track. Optoelectronics Letters, 18, 434-439. https://doi.org/10.1007/s11801-022-2013-x

[16] Liu, Z., Kim, J. I., & Yoo, W. S. (2024). Decision support for railway track facility management using openbim. Automation in Construction, 168(Part B), 105840. https://doi.org/10.1016/j.autcon.2024.105840

[17] Wang, N. X., Zhao, H. K., He, Q. J., & Zheng, G. S. (2025). Blind source separation LTE-M co-channel interference detection based on vector weighted average optimization. Industrial Control Computer, 38(2), 45-47. https://doi.org/10.3969/j.issn.1001-182X.2025.02.017

[18] Thelaidjia, T., Chetih, Nabil., Moussaoui, Abdelkrim., & Chenikher, Salah. (2023). Successive variational mode decomposition and blind source separation based on salp swarm optimization for bearing fault diagnosis. The International Journal of Advanced Manufacturing Technology, 125, 5541-5556. https://doi.org/10.1007/s00170-023-10968-3

[19] Koohmishi, M., Kaewunruen, S., He, X., & Guo, Y. (2025). Advancing railway sustainability: strategic integration of circular economy principles in ballasted track systems☆. Journal of Cleaner Production, 490, 144713. https://doi.org/10.1016/j.jclepro.2025.144713

[20] Li, Z. Y., Li, X. F., Yao, R. G., Zhang, S. J., Xie, Y., & Zuo, X. Y. (2025). An accelerated underdetermined blind source separation algorithm based on tensor decomposition. Journal of Signal Processing, 41(3), 515-523. http://dx.doi.org/10.12466/xhcl.2025.03.009